Section 5 VLER Lattice and Optics

The VLER storage ring has been designed in order to meet the following requirements:

- to operate with an energy variable between 150 and 500 MeV;
- to provide the flexibility to tune the sum of the beam emittances between 300 and 600 nm, while varying the energy;
- to collide with LER without perturbing the Babar operation;
- to fit in the Hall 12, leaving enough space for the injection line from the Linac;
- to allow for head-on collisions with a minimum impact on the detector;
- to have reasonable lifetimes.

All these requirements are fulfilled by the present design. The ring circumference was chosen to be a multiple of the LER bunch spacing. However we could not choose a VLER length that is a sub-multiple of the LER length, so the e^- bunches will collide with many different e^+ bunches. The possible implications of this choice was addressed in the beam-beam studies Sec. 3.

LATTICE DESIGN

The ring has a two-fold symmetry with a circumference of 35.27 m. This is 28 times the LER by 2 bunch spacing. The beams collide head-on and the detector magnetic field is part of the VLER Interaction Region. To minimize both space and cost a pentagon-like shape has been chosen where all the arc dipoles have the same field. The layout is sketched in Fig. 5-1.

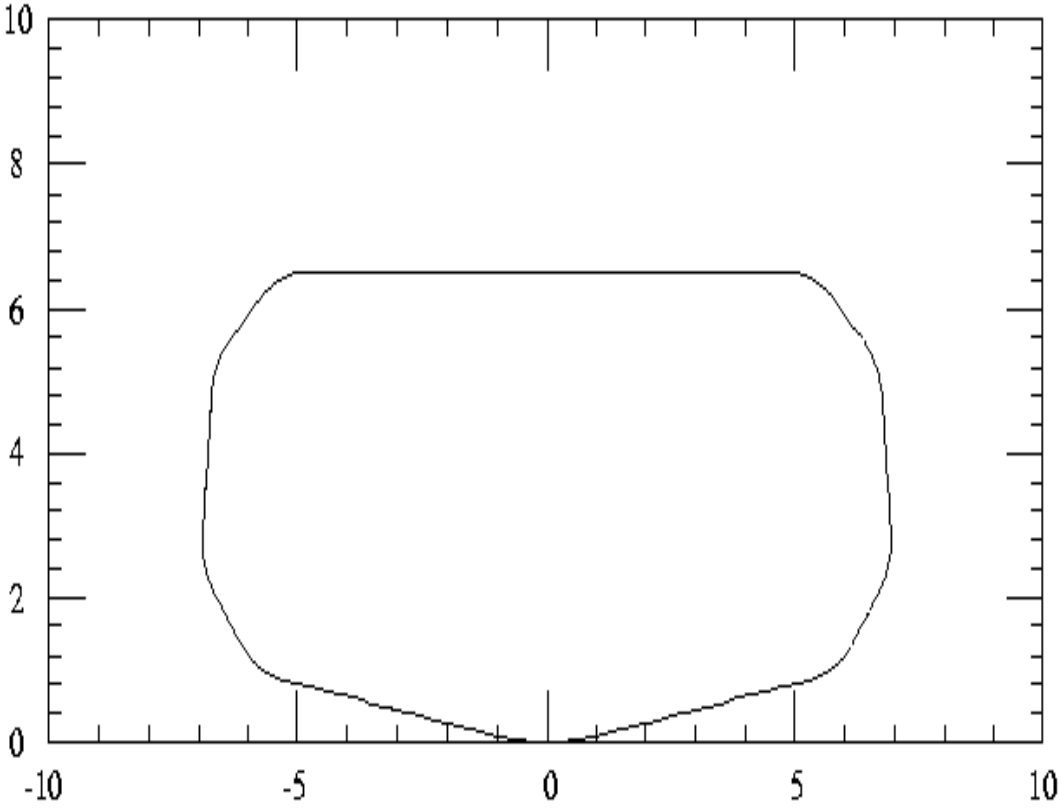

Fig. 5-1: Ring Layout in meters. The IP is located at 0.

The lattice consists of two straight sections and two arcs. In the IP straight the beam will collide with the LER beam and the other straight contains injection kickers, septum, feedback kickers and one RF cavity. The focusing at the IP and along the IP straight is provided by two QD-QF doublets, symmetric with respect to the IP. In the injection straight there are also two QD-QF doublets, which allow the ring optical functions to be symmetric with respect to the straight midpoint. The horizontal dispersion vanishes at the IP as well as in the RF/injection region. The IP beta functions were chosen in order to optimize both luminosity and beam-beam tune shifts: β_x^* = .37 m, β_y^* = .03 m. The maximum β_y is about 80. m in QDI1, and the maximum β_x is about 50. m in QFI1. A more detailed description of the IP straight was given in Sec.4.

Due to the limited available space, a FODO cell solution as in the LER and HER arcs was not easily feasible. A compact arc design has been chosen which allows for both emittance tunability (from 300 to 600 nm, horizontal, off-coupling) and dispersion suppression in the RF/injection straight. Each arc houses four 0.9 m long dipoles each with a bending angle of 42.42˚

and a field of 1.37 T at 500 MeV, interleaved with 5 quadrupoles. The total number of normal conducting quadrupoles in the ring is 20, while the two closer to the IP are of permanent magnets type. The total number of dipoles is 8 plus the IP magnet. Because of the ring symmetry the quadrupoles will be powered in pairs, to allow maximum lattice flexibility.

For three energies (500, 300 and 150 MeV) a "low" emittance lattice (ε_x = 300 nm, off-coupling) and a "high" emittance lattice (ε_x = 600 nm, off-coupling) were studied. The need to keep the emittance constant is suggested by beam-beam considerations (see Sec.3).

Four families of sextupoles have been foreseen: three in the arcs for chromaticity correction, and one in the injection straight to correct the beam tune shift with amplitude. Some space is also available for closed orbit correctors and emittance-coupling skew quadrupoles.

In Table 5-1 the main lattice parameters are summarized. Depending on the working energy and emittance we will have six different lattices, and then six quadrupole and sextupole settings. For each case the minimum and maximum possible values of the parameter are shown. In Table 5-2 the magnetic layout is reported for one half of the ring. Dipole fields and quadrupole and sextupole gradients refer to the maximum energy of 500 MeV and the off-coupling emittance of 300 nm. Optical functions are presented in Figures 5-2 to 5-7 for each case studied.

Table 5-1: Main Lattice Parameters

E (MeV)	150 - 500.	**C (m)**	35.27
f_{rev} (MHz)	8.5	**h**	56
β_x* (m)	0.37	**β_y* (m)**	0.03
Max IR β_x (m)	60.	**Max IR β_y (m)**	80.
Max Arc β_x (m)	18.- 65.	**Max Arc β_y (m)**	20. - 50.
η_x* (m)	0.0	**Max η_x (m)**	1.3 - 2.
σ_x* (mm)	.26 - .37	**σ_y* (μm)**	34. - 83.
ε_x (nm) off coupling	300- 600	**k = ε_y / ε_x**	.55 - .64
α_c	.07 - .09	**σ_l (cm) @100kV**	.3 - 1.2
X-chromaticity	-18 - -10	**Y-chromaticity**	-22 - -16
$\sigma_E/E * 10^{+4}$	1.1 - 3.9	**U_0 (keV/turn)**	.04/4.6
τ_x (ms)	1500. - 45.	**τ_y (ms)**	1000.- 27.
τ_E (ms)	400. - 12.	**ν_s @100 kV**	.012 - .02

Table 5-2: Layout of one half of ring for E = 500 MeV, ε_x = 300 nm

	L (m)	Total L (m)	Quad/Sxt strength (m^{-2})	Quad/Sxt Gradient (T/m)/(T/m^2)	Quad/Sxt Int. Grad (T)/(T/m)	Dipole angle (°)	Dipole radius (m)	Dipole field (T)
B0	1.	1.				10.313	5.5555	0.3
DRIFT	0.5	1.5						
QDI1	0.2	1.7	-5.2	8.67	1.73			
DRIFT	0.8	2.5						
QFI1	0.3	2.8	+4.1	6.83	2.05			
DRIFT	0.5	3.3						
QDI2	0.3	3.6	-2.95	4.92	1.48			
DRIFT	0.6	4.2						
QFI2	0.3	4.5	+1.25	2.10	0.63			
DRIFT	0.96	5.46						
BEND	0.9	6.36				42.42	1.2155	1.37
DRIFT	0.3	6.66						
QF5	0.3	6.96	+2.6029	4.34	1.3			
DRIFT	0.3	7.26						
BEND	0.9	8.16				42.42	1.2155	1.37
DRIFT	0.1	8.26						
SD1	0.1	8.36	-12.	200.	20.			
DRIFT	0.1	8.46						
QD6	0.2	8.66	-4.	6.67	1.33			
DRIFT	0.1	8.76						
SF2	0.1	8.86	+14.	233.3	23.3			
DRIFT	0.1	8.96						
QF7	0.3	9.26	+5.2882	8.81	2.64			
DRIFT	0.3	9.56						
QD8	0.2	9.76	-4.4	7.33	1.47			
DRIFT	0.1	9.86						
SD3	0.1	9.96	-18.7	311.7	31.17			
DRIFT	0.1	10.06						
BEND	0.9	10.96				42.42	1.2155	1.37
DRIFT	0.3	11.26						
QF9	0.3	11.56	+3.9576	6.60	1.98			
DRIFT	0.3	11.86						
BEND	0.9	12.76				42.42	1.2155	1.37
DRIFT	0.15	12.91						
SD4	0.1	13.01	-4.	66.7	6.67			
DRIFT	0.15	13.16						
QD10	0.3	13.46	-2.2390	3.73	1.12			
DRIFT	1.4	14.86						
QF11	0.3	15.16	+1.1826	1.97	0.59			
DRIFT	2.475	17.635						

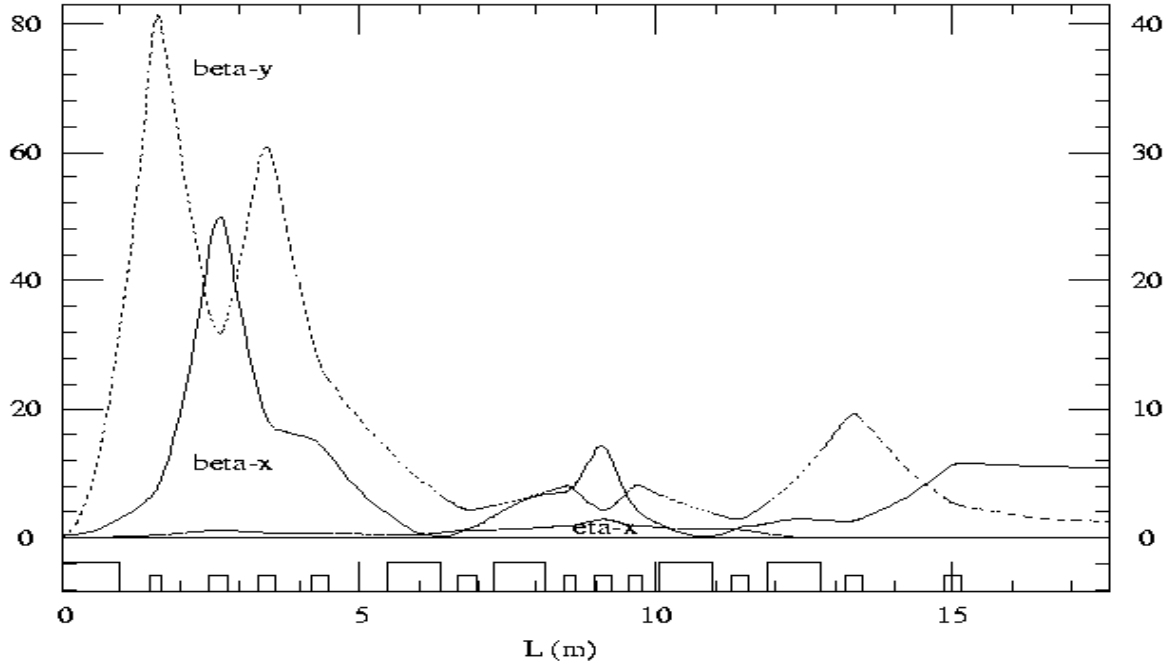

Fig.5-2: Optical functions for E = 500 MeV and ε_x = 300 nm.

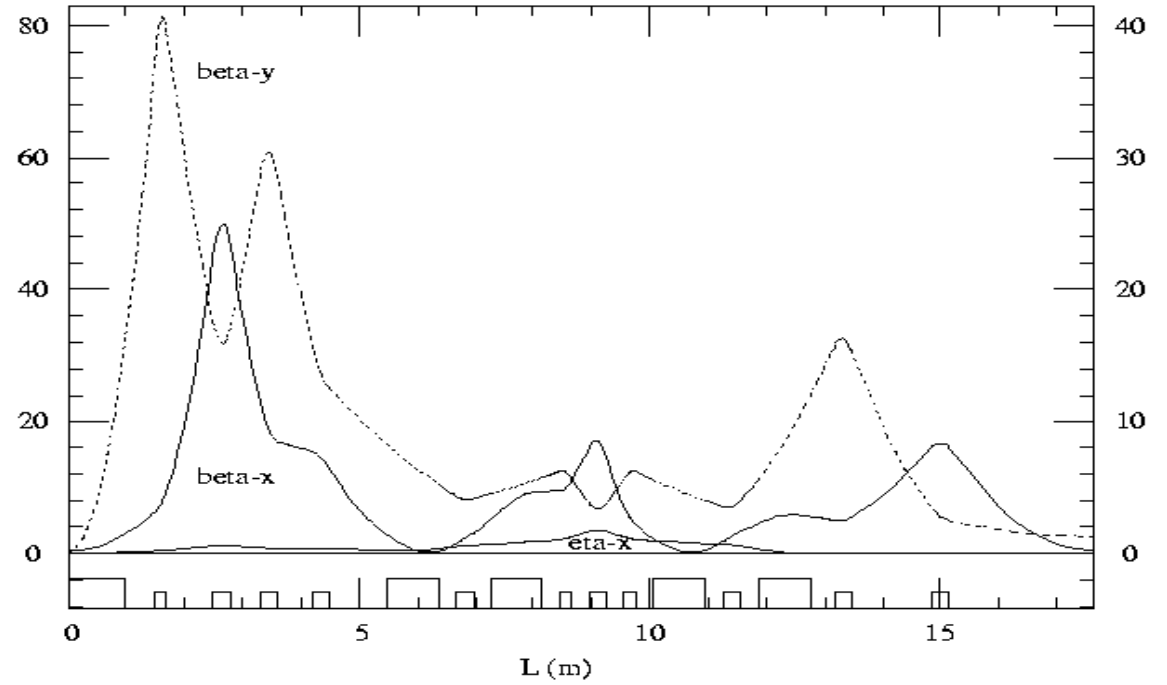

Fig.5-3: Optical functions for E = 500 MeV and ε_x = 600 nm.

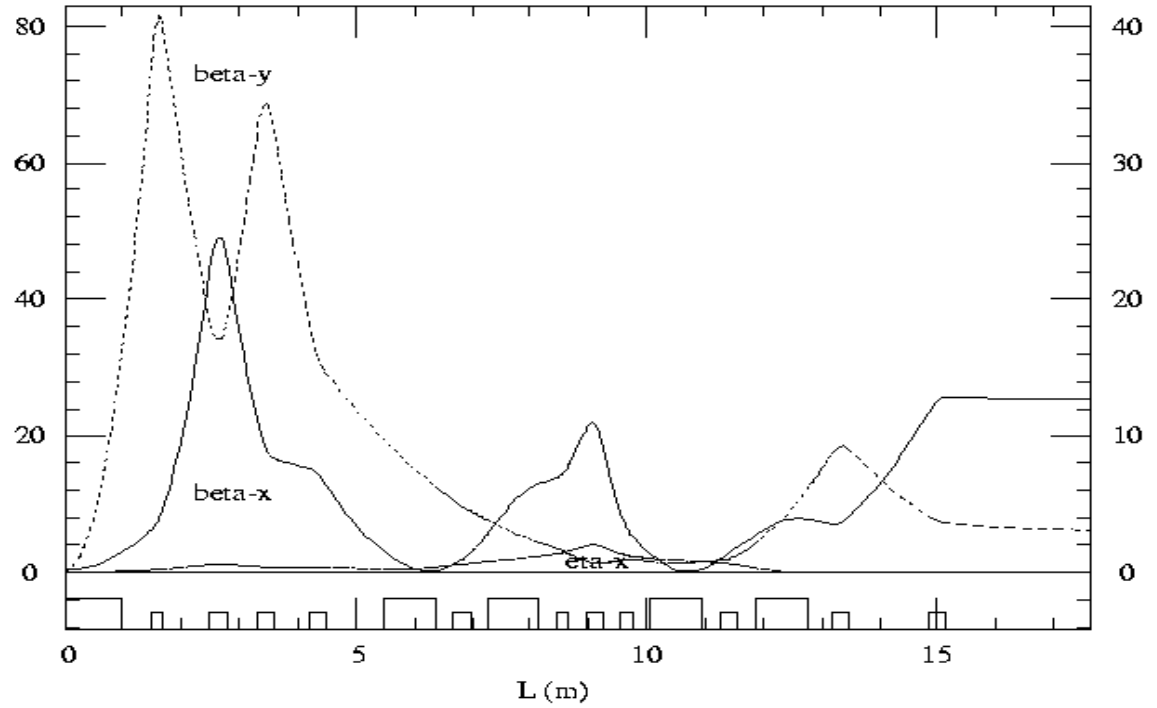

Fig.5-4: Optical functions for E = 300 MeV and ε_x = 300 nm.

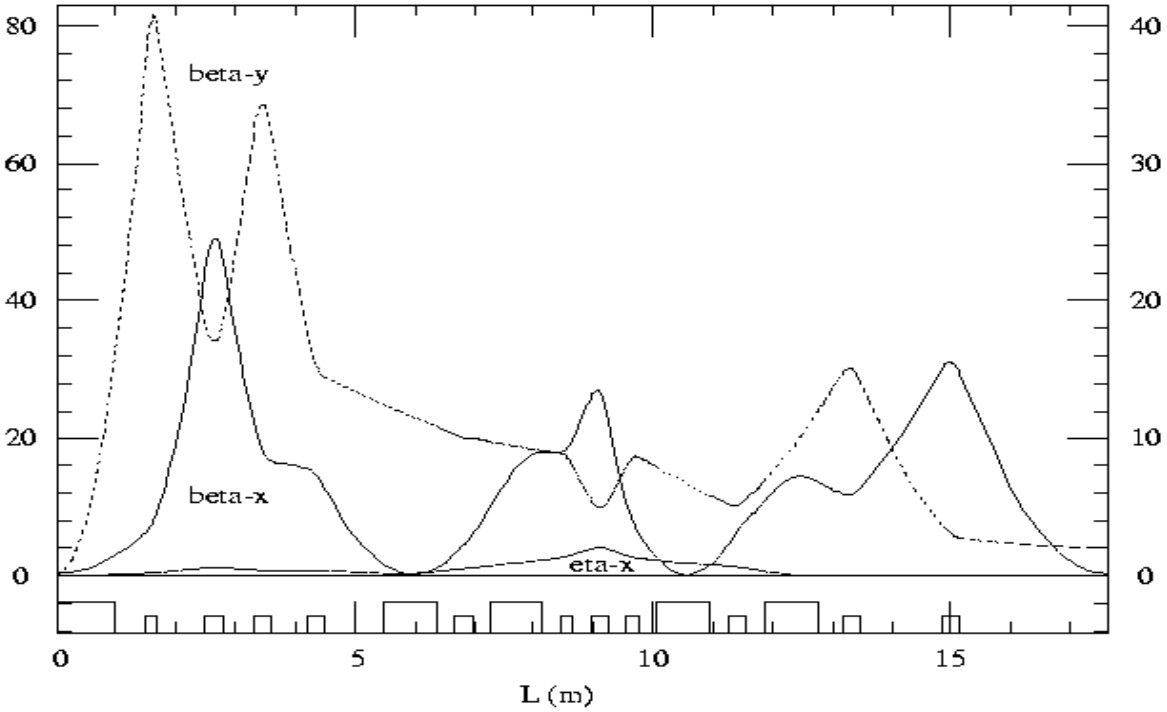

Fig.5-5: Optical functions for E = 300 MeV and ε_x = 600 nm.

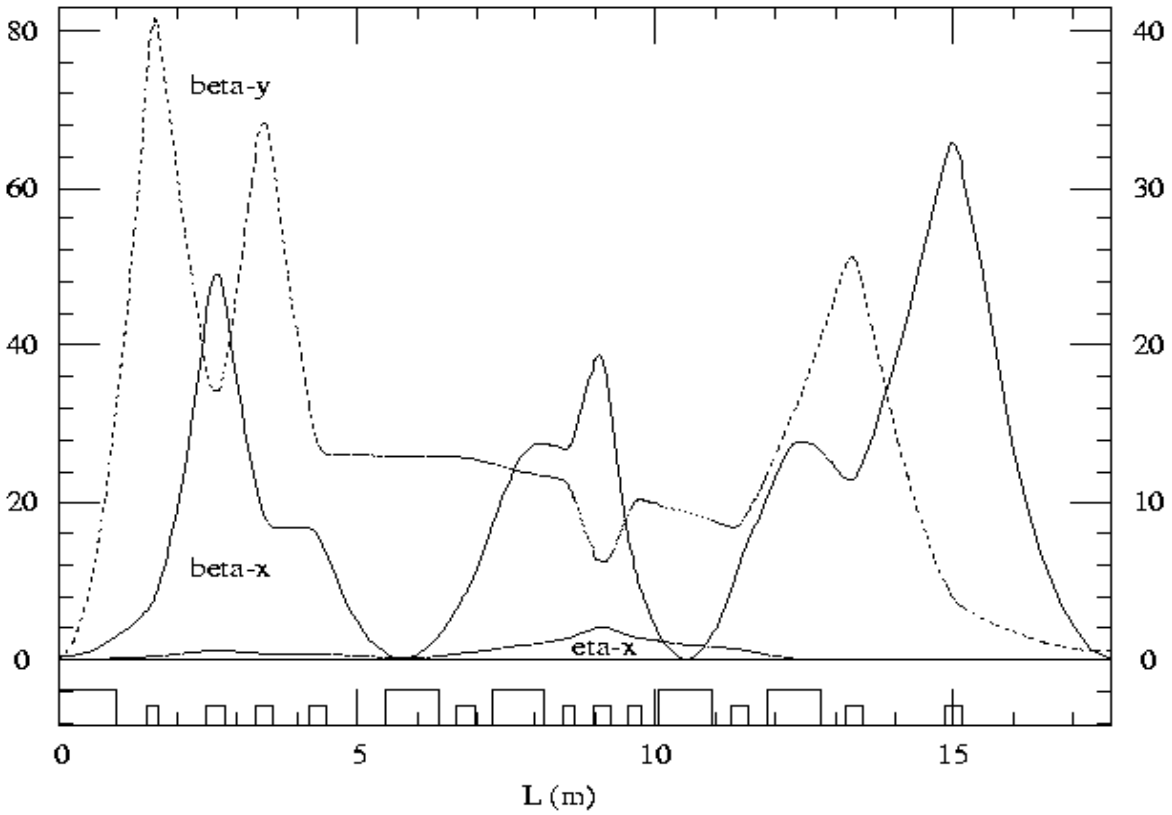

Fig.5-6: Optical functions for E = 150 MeV and ε_x = 300 nm.

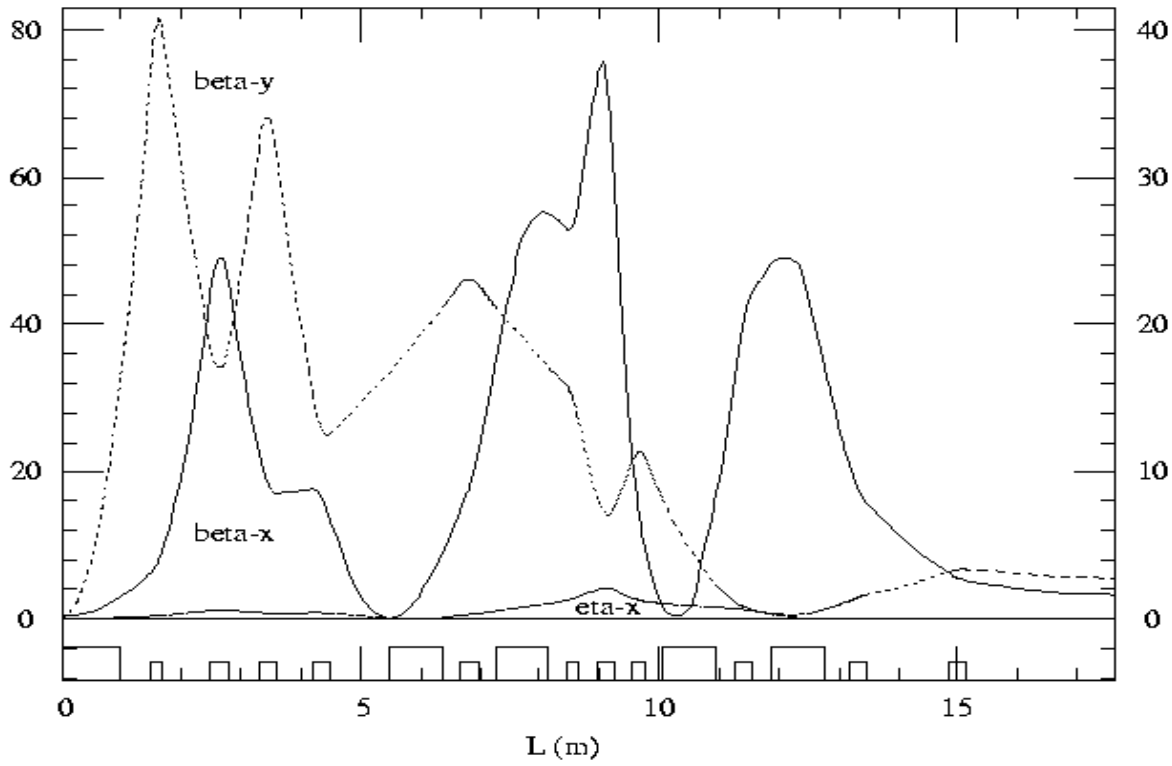

Fig.5-7: Optical functions for E = 150 MeV and ε_x = 600 nm.

DYNAMIC APERTURE STUDIES

A preliminary study of the dynamic aperture with a fast tracking program has been performed for the (500 MeV, 300 nm) lattice and IP nominal beta functions. The horizontal and vertical chromaticities have been corrected to zero by means of three sextupole families located in the arcs, in regions were the betatron functions in the two planes are quite well separated and the dispersion is maximum. Due to the low value of β_y^*, the vertical chromaticity is about a factor of two higher than the horizontal in this configuration. For this reason two families have been used to correct the vertical chromaticity and one for the horizontal. The sextupole arrangement has a reflected symmetry with respect to the RF/injection straight midpoint. The resulting sextupole strengths are reasonable, but due to space issues the phase shifts between sextupoles are presently not optimized to exactly cancel chromatic and geometric aberrations.

Particles with initial conditions confined in a region of ($\pm 10\ \sigma_x^*$, $+10\ \sigma_y^*$) at nominal coupling, and for three fixed energy deviations, corresponding to $\Delta p/p = (-10\ \sigma_E/E,\ 0,\ +10\ \sigma_E/E)$, were tracked for 1024 turns. Magnet errors and synchrotron oscillations have not yet been studied. The resulting stable area for on-energy and off-energy tracking is shown in Fig. 5-8, where each star represents a particle stable after 1024 turns. The results look promising since the stable area is larger than $\pm 10\ \sigma_x$ both for on-energy and off-energy particles and the only unstable motion seems to occur for large negative horizontal amplitudes associated with large ($>8\ \sigma_y$) vertical amplitudes.

In Fig. 5-9 the fractional part of the horizontal and vertical tunes as a function of the particle momentum is plotted. There is evidence of a small non linear behavior in the vertical tune.

In Fig. 5-10 the fractional part of the horizontal and vertical tunes as a function of the particle initial amplitudes are plotted. In abscissa are the horizontal and vertical amplitudes expressed in number of σ_x or σ_y. Both tune behaviors seem quite flat. One family of vertical

focusing sextupole in a dispersion free region was used to correct the vertical tune shift for large vertical amplitudes.

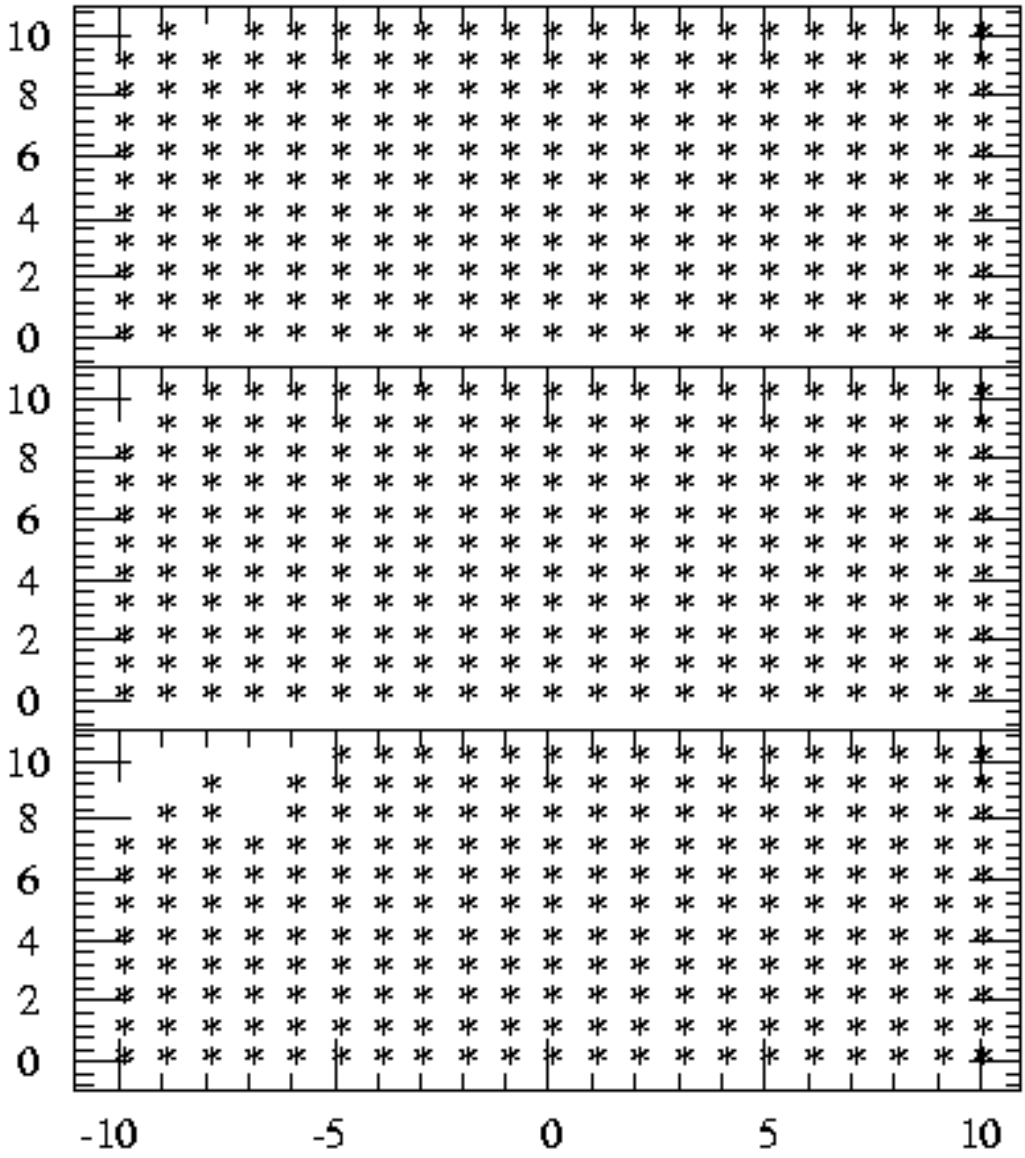

Fig 5-8: Dynamic aperture for E = 500 MeV and ε_x = 300 nm. In abscissa and ordinata are the particle initial horizontal and vertical amplitudes at the IP in # of sigmas.

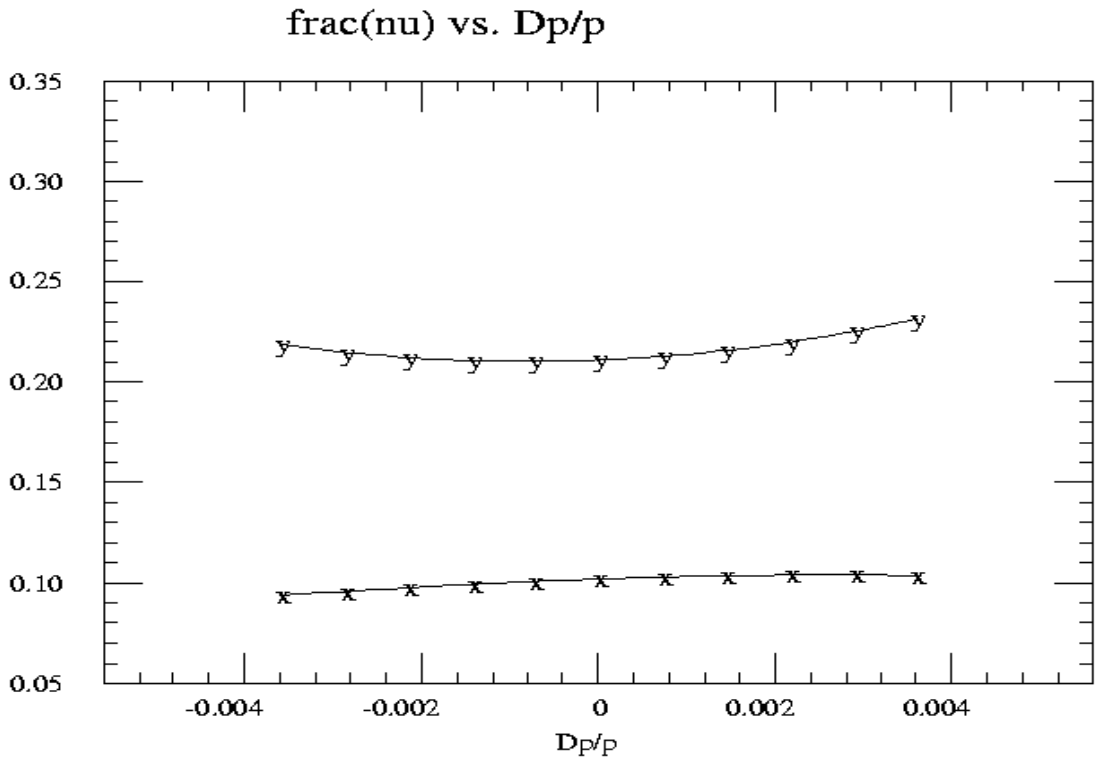

Fig. 5-9: Horizontal (x) and vertical (y) tune variation as a function of the particle momentum deviation.

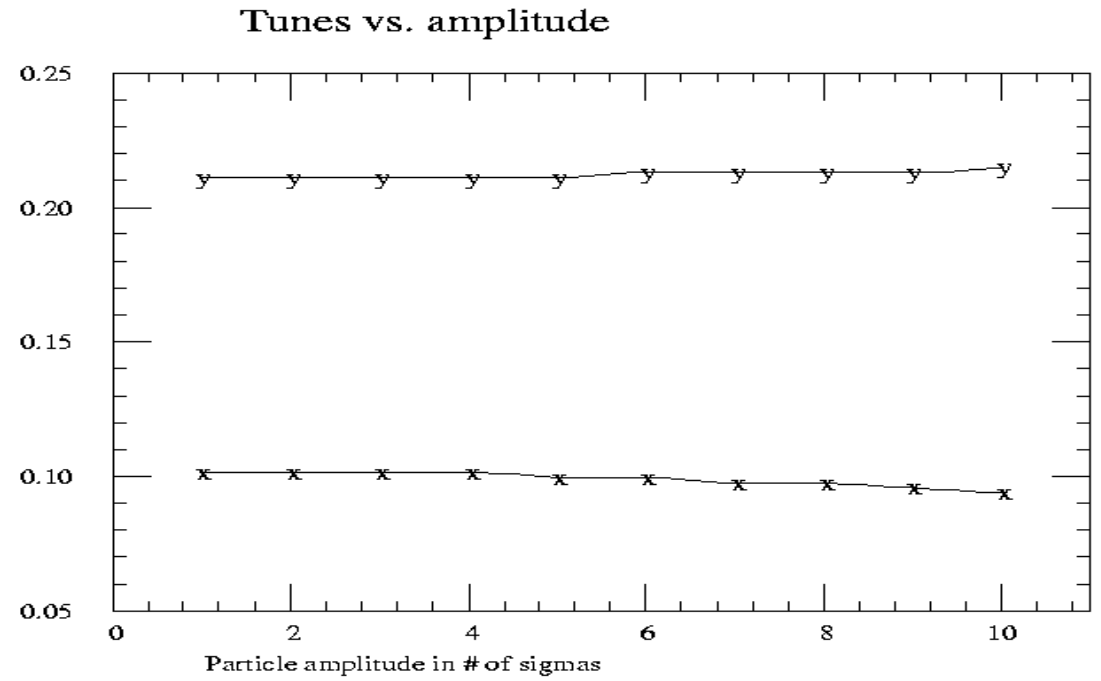

Fig. 5-10: Horizontal (x) and vertical (y) tune variation as a function of the amplitude in # of horizontal and vertical sigmas.